Coastal Engineering 57 (2010) 694–708 Elsevier B.V. doi:10.1016/j.coastaleng.2010.02.009

Elsevier Editorial System(tm) for Coastal Engineering
Manuscript Draft

Manuscript Number: CENG-D-08-00111R2

Title: Changes in Venice Lagoon dynamics due to construction of mobile barriers

Article Type: Case Study

Keywords: MoSE Project; hydrodynamic model; mobile barriers; Venice Lagoon

Corresponding Author: Mrs Michol Ghezzo,

Corresponding Author's Institution:

First Author: Michol Ghezzo

Order of Authors: Michol Ghezzo; Stefano Guerzoni; Andrea Cucco; Georg Umgiesser

Abstract: The Mo.S.E. project (construction of mobile barrier to safeguards the lagoon of Venice) entails changes to the structure of the lagoon's inlets. This could have consequences for the areas near the inlets and for the dynamics of the lagoon ecosystem as a whole. In order to predict the effects of the proposed alterations on the hydrodynamics of the lagoon, a well-tested hydrodynamic-dispersion model was applied. Simulations were carried out considering both idealised and realistic tide and wind scenarios.

The results show that with the new structures the Lido subbasin tends to increase his extension due the southward movement of the watershead, at the expense of the Chioggia subbasin, whereas the Malamocco subbasin can change his relative position, but not his extension.

The residence time shows variations in agreement with this trend, decreasing in the southern part of Lido subbasin and increasing in the inner part of the Chioggia subbasin.

The variations of residence time and return flow factor indicate that the responsable of those effects are the changes both in the instantaneous velocity currents and in the sea-lagoon interaction. In fact the new breakwaters in front of the Malamocco and Chioggia inlets modify the length and direction of the outflow jet (up to 1 m/s) and the patterns of the currents around the inlets and the nearby coast.

The new artificial island in the Lido inlet changes the current pattern and increases the current velocity on the southern side of the channel propagating this effect up to the Venice city.

The risks and benefits individuated from our conclusion are that the Lido subbasin can improve his renewal time but the more intense current speeds can be a risk for habitats and infrastructures conservation. Finally the microcirculation between the breakwater and the coast in Chioggia and Malamocco inlets can be a trap for pollutants or suspended sediment.

Changes in Venice Lagoon dynamics due to construction of mobile barriers.

Michol Ghezzo[a,*], Stefano Guerzoni[1], Andrea Cucco[b], Georg Umgiesser[a]

[a] *Institute of Marine Science - National Research Council (ISMAR-CNR), Castello 1364/a, 30122, Venice, Italy.*

[b] *Institute for the Coastal Marine Environment - National Research Council (IAMC-CNR), Oristano, Italy*

Abstract

The MoSE project (construction of mobile barrier to safeguards the lagoon of Venice) entails changes to the structure of the lagoon's inlets. This could have consequences for the areas near the inlets and for the dynamics of the lagoon ecosystem as a whole. In order to predict the effects of the proposed alterations on the hydrodynamics of the lagoon, a well-tested hydrodynamic-dispersion model was applied. Simulations were carried out considering both idealised and realistic tide and wind scenarios.

The results show that with the new structures the Lido subbasin tends to increase its extension due the southward movement of the watershed, at the expense of the Chioggia subbasin, whereas the Malamocco subbasin changes its relative position, but not its extension.

The residence time shows variations in agreement with this trend, decreasing in the southern part of the Lido subbasin and increasing in the

*Corresponding author. Phone.: +39-041-2404758, FAX: +39-041-5204126

Email addresses: michol.ghezzo@ve.ismar.cnr.it (Michol Ghezzo), stefano.guerzoni@ve.ismar.cnr.it (Stefano Guerzoni), andrea.cucco@iamc.cnr.it (Andrea Cucco), georg.umgiesser@ismar.cnr.it (Georg Umgiesser)

inner part of the Chioggia subbasin.

The variations of residence time and return flow factor indicate that the responsible of those effects are the changes both in the instantaneous current velocities and in the sea-lagoon interaction. In fact the new breakwaters in front of the Malamocco and Chioggia inlets modify the length and direction of the outflow jet (up to 1 m s^{-1}) and the patterns of the currents around the inlets and the nearby coast. The new artificial island in the Lido inlet changes the current pattern and increases the current velocity on the southern side of the channel propagating this effect up to the Venice city.

The risks and benefits individuated from our conclusion are that the Lido subbasin can improve its renewal time, but the more intense current speeds can be a risk for the conservation of habitats and infrastructures. Finally the micro-circulation between the breakwater and the coast in Chioggia and Malamocco inlets can be a trap for pollutants or suspended sediment.

Keywords: MoSE Project, hydrodynamic model, mobile barriers, Venice Lagoon

1. Introduction

The Venice lagoon is located in the northwest Adriatic Sea. It is a large lagoon (500 km^2 in area, 50 km in length) with a complex bathymetry characterised by a network of channels, flats and shoals (Molinaroli et al., 2007). Water exchange between the lagoon and the northern Adriatic Sea takes place through three inlets situated on the eastern side of the lagoon. These inlets are named, from north to south, Lido, Malamocco and Chioggia. The first is around 1000 m wide, and the others about 500 m. The maximum depth is around 8 m for Chioggia and 14 m for Malamocco and Lido.

Most of the lagoon is very shallow, with average depths in the order of 1 m, but there are also a few deep channels (maximum depth around 15 m) leading inwards from each inlet and branching inside the basin. Traditionally the lagoon is subdivided into three sub-basins, one for each inlet, separated by two watersheds through which the residual flow is minimum (Solidoro et al., 2004). The exchange of water through the inlets in each tidal cycle is about a third of the total volume of the lagoon (Gacic and Solidoro, 2004). The main circulation forcing factors are the tide (± 50 cm during spring tide) and the wind. Stratification of water masses is seen only at some distance from the inlets, where the tidal energy is low. Inside the inlets, water velocities are high (over 1 m s^{-1}) and the vertical shear creates enough turbulence to mix the water column. Consequently, water exchanges between the lagoon and the sea are essentially barotropic (Gacic et al., 2002).

The MoSE project (from the Italian acronym for Experimental Electromechanic Module, short description in `http://www.veniceword.com/news/8/mose.html`) is a long-debated project (Nosengo, 2003; Bras et al., 2001; Ammerman and McClennen, 2000) to defend the city of Venice and the surrounding lagoon from "high water" events. The project entails building mobile barriers at the bottom of each inlet which, when tidal events threaten to become critical, will rise and shut off the lagoon from the sea.

At the time of writing the project is still being implemented, and the configuration and bathymetries of the three lagoon inlets are being altered. These changes are likely to modify the interactions between the lagoon and the sea, the local hydrodynamics around the inlets, and the general circulation of the lagoon basin. All these aspects could have direct and indirect effects on the Sites of Community Interest (SCIs) around the inlets and on the quality of the lagoon environment as a whole (Spiro and Rizzardi, 2006).

The available literature includes studies of various aspects of the MoSE project: the department of Hydraulics of Padua University (IMAGE - Padua University, 2006) analysed the hydrodynamic effects of various inlet configurations. Berrelli et al. (2006) explored the dynamics of the basin under different wind forcing scenarios and predicted the possible consequences of the mobile barrier closures. Umgiesser and Matticchio (2006) considered the potential negative effects of the MoSE project on commercial activity in Venice harbour. Rosatti et al. (2002) examined the effects of the mobile barriers on the transport of a passive pollutant. Bendoricchio and De Boni (2005) used a statistical model to quantify the effects on water quality.

Several investigations have been carried out in the past to evaluate the effect of different inlets structures on the tide levels inside the lagoon. The methods employed are the analysis of measurements (Pirazzoli, 2004), or the application of numerical models (Umgiesser, 1999; Maticchio, 2004; Benetazzo, 2004). Other works handle theoretical aspects on the application of numerical models (Delfina, 2004), or evaluate the effect of different arrangement of the inlets and of the lagoon on its residence time (Umgiesser, 2004). The configuration of the inlets, to which most of these studies are referred, has been recently changed, and in the previous modelling implementations simplified forcings, domains and set-ups have been chosen.

No investigations have yet been carried out, with the inlet structure recently projected, of the effects on water circulation in the Venice lagoon resulting from modifications of the inlet structure in itself. Only Mosquera et al. (2007) analysed the time-series of estimated monthly mean flows through the inlets and highlights the increased amplitude of the three tidal constituents in Chioggia inlet, starting from the second half of the year 2004; he suggests the possible impact of inlet narrowing on water flows.

After the MoSE project is completed, the most common situation in the Venice lagoon will be one in which the new structures have been installed - thus changing the configuration of the seaward inlets - but are not in operation. The effects of this new inlet configuration are an important aspect of the question.

In this study, numerical modelling techniques were applied in order to predict the consequences for lagoon hydrodynamics of modifications to the geometry of the inlets. This approach makes it possible to analyse various spatial and temporal scales and verify local and global effects on the lagoon's dynamics. In addition, numerical modelling enables calculation of complex indices, such as residence times, which characterise the behaviour of the lagoon.

A coupled hydrodynamic and tracer-transport model was applied. Several simulations were carried out in order to compare the results obtained using two different numerical grids representing the post and ante operam configurations of the inlets, and to contrast the responses of the new and old configurations under different environmental forcing scenarios.

2. Methods

2.1. The SHYFEM hydrodynamic model

The SHYFEM model is a hydrodynamic model developed at ISMAR-CNR and applied successfully in the Venice lagoon and in numerous coastal basins (Umgiesser, 2000; Melaku Canu, 2001; Umgiesser et al., 2004; Ferrarin and Umgiesser, 2005; Cucco et al., 2006; Zemlys et al., 2008; Ferrarin et al., In Press; Cucco et al., 2009). For spatial integration the model uses finite elements in the horizontal discretization and z-layers in the vertical discretization and a semi-implicit algorithm for integration in time. The finite element method allows high flexibility in spatial domain discretization, because it makes it possible to employ elements with different shapes and sizes. This is an important feature for representing the complex geometries that are typical of shallow water basins such as the lagoon of Venice.

The model is able to consider flooding and drying of shallow water flats. In the Venice lagoon, 15% of the area is subject to partial flooding and drying during the spring tide cycle. The mechanism used to represent this phenomenon has been implemented in a mass-consistent way without the negative effects of spurious oscillations (Umgiesser and Bergamasco, 1993; Umgiesser et al., 2004). Numerically, the divergence terms in the continuity equation, together with the Coriolis term, and the barotropic pressure gradient in the momentum equation, are treated semi-implicitly. The vertical stress terms and the bottom friction term are treated fully implicitly, while all other terms (horizontal diffusion and advective terms in the momentum equations) are treated fully explicitly. This discretization provides unconditional stability with regard to the effects of fast gravity waves, bottom friction and Coriolis acceleration (Umgiesser and Bergamasco, 1995). The 3D-equations integrated over each layer read as follows:

$$\begin{aligned}\frac{\partial U_l}{\partial t} + Adv^x{}_l - fV_l = -gh_l\frac{\partial \zeta}{\partial x} - \frac{gh_l}{\rho_0}\frac{\partial}{\partial x}\int_{-H_l}^{\zeta}\rho^{'}dz + \\ -\frac{h_l}{\rho_0}\frac{\partial p_a}{\partial x} + \frac{1}{\rho_0}(\tau_x{}^{top(l)} - \tau_x{}^{bottom(l)}) + A_H\left(\frac{\partial^2 U_l}{\partial x^2} + \frac{\partial^2 U_l}{\partial y^2}\right)\end{aligned} \quad (1)$$

$$\begin{aligned}\frac{\partial V_l}{\partial t} + Adv^y{}_l + fU_l = -gh_l\frac{\partial \zeta}{\partial y} - \frac{gh_l}{\rho_0}\frac{\partial}{\partial y}\int_{-H_l}^{\zeta}\rho^{'}dz + \\ -\frac{h_l}{\rho_0}\frac{\partial p_a}{\partial y} + \frac{1}{\rho_0}(\tau_y{}^{top(l)} - \tau_y{}^{bottom(l)}) + A_H\left(\frac{\partial^2 V_l}{\partial x^2} + \frac{\partial^2 V_l}{\partial y^2}\right)\end{aligned} \quad (2)$$

$$\frac{\partial \zeta}{\partial t} + \sum_l \frac{\partial U_l}{\partial x} + \sum_l \frac{\partial V_l}{\partial y} = 0 \quad (3)$$

where

$$Adv^x{}_l = u_l\frac{\partial U_l}{\partial x} + v_l\frac{\partial U_l}{\partial y} \qquad Adv^y{}_l = u_l\frac{\partial V_l}{\partial x} + v_l\frac{\partial V_l}{\partial y} \quad (4)$$

In the previous equations l indicates the vertical layer (1 for the surface), (U_l, V_l) the horizontal velocities integrated over the layer (transports), and (u_l, v_l) the velocities in x and y directions, p_a is the atmospheric pressure, g the gravitational constant, f the Coriolis parameter, ζ the water level, ρ_0 the constant water density, $\rho = \rho_0 + \rho^{'}$ the water density, h_l the layer thickness, H_l the depth of the bottom of the layer l, A_H the horizontal eddy viscosity. The stress terms are expressed as:

$$\tau_x^{top(l)} = \rho_0\nu_l\frac{(u_{l-1} - u_l)}{(h_{l-1} + h_l)/2} \qquad \tau_x^{bottom(l)} = \rho_0\nu_l\frac{(u_l - u_{l+1})}{(h_l + h_{l+1})/2} \quad (5)$$

$$\tau_y^{top(l)} = \rho_0\nu_l\frac{(v_{l-1} - v_l)}{(h_{l-1} + h_l)/2} \qquad \tau_y^{bottom(l)} = \rho_0\nu_l\frac{(v_l - v_{l+1})}{(h_l + h_{l+1})/2} \quad (6)$$

where ν_l is the vertical viscosity for layer l computed with a $k-\varepsilon$ model. The boundary conditions for the stress terms are:

$$\tau_x^{surface} = c_D \rho_a w_x \sqrt{w_x{}^2 + w_y{}^2} \qquad \tau_y^{surface} = c_D \rho_a w_y \sqrt{w_x{}^2 + w_y{}^2} \tag{7}$$

$$\tau_x^{bottom} = c_B \rho_0 u_L \sqrt{u_L{}^2 + v_L{}^2} \qquad \tau_y^{bottom} = c_B \rho_0 v_L \sqrt{u_L{}^2 + v_L{}^2} \tag{8}$$

where c_D is the wind drag coefficient, c_B the bottom friction coefficient, ρ_a the air density, (w_x, w_y) the wind velocity and u_L, v_L the bottom velocity The bottom drag coefficient c_B is assumed to be constant and the bottom friction term has a quadratic formulation.

At the open boundary, the water levels are prescribed in agreement with the Dirichlet condition, while at the closed boundaries only the normal velocity is set to zero and the tangential velocity is a free parameter. This corresponds to a full slip condition, and considering that in this study the smallest elements are of the order of 10 m, it is a good approximation.

Although horizontal temperature and salinity gradients exist in the lagoon, giving rise to baroclinic pressure terms, the barotropic pressure gradient is much stronger close to the inlet areas, as explained in the introduction and pointed out by other authors (Bellafiore et al., 2008; Gacic et al., 2002). Umgiesser et al. (2004) demonstrated, through a scale analysis that, for the Lagoon of Venice, the barotropic pressure gradients are an order of magnitude bigger than the baroclinic ones. Studies of other authors (Bellafiore et al., 2009; Ferrarin et al., In Press) and several tests carried out for the present study pointed out that a three dimensional model is needed to adequately describe the discharges through the inlets. Therefore, the model has been applied in its 3D version, but the baroclinic pressure terms have been neglected.

The SHYFEM model is coupled with the transport and diffusion of a passive tracer module, which simulates the temporal and spatial evolution of the concentration of a dissolved tracer in the water column, in accordance with the following equation:

$$\frac{\partial s_l}{\partial t} + \frac{\partial u_l s_l}{\partial x} + \frac{\partial v_l s_l}{\partial y} + \frac{\partial w_l s_l}{\partial z} = \frac{\partial}{\partial x}(K_H \frac{\partial s_l}{\partial x}) + \frac{\partial}{\partial y}(K_H \frac{\partial s_l}{\partial y}) + \frac{\partial}{\partial z}(\nu_l^W \frac{\partial s_l}{\partial z}) \quad (9)$$

where s_l is the tracer concentration over layer l, u_l and v_l are the velocities in the layer and K_H and ν_l^W are the horizontal and the vertical eddy diffusivities respectively: the horizontal diffusivity is computed by Smagorinsky's formulation with a coefficient of 0.2, and the vertical by a $k - \varepsilon$ model. Fluxes between the bottom and the water column are not considered here.

2.2. The numerical grid

Numerical simulations were carried out on two distinct finite element grids, which represent the different geometrical set-ups of the lagoon inlets before (ante operam) and after (post operam, Fig. 1) the modifications of the inlets.

The numerical grid used to reproduce the lagoon basin geometry and bathymetry ante operam is made up of 28900 elements and 15250 nodes. The smallest elements are near the deep narrow channels and around the inlets. The average spatial resolution in the inlet area ranges from 50 to 10 m. The numerical grid adopted to reproduce the geometry of the lagoon post operam represents the configuration of the inlets after the installation of the new structures. It was obtained by modifying elements of ante operam grid lying along the new perimeter resulting from the changed structure of the inlets. The two meshes are therefore nearly identical and have almost the same total number of nodes and elements. Both grids extend outside the lagoon up to 30 km offshore, in order to minimize the influence of the open boundary. The offshore border of the numerical grids is considered an open boundary, whereas the lagoon and coastal areas are treated as closed boundaries.

The bathymetric data adopted in the ante operam grid were collected in the year 2000, whereas in the post operam grid the bathymetry of the inlets follows the depth values specified in the plans of the MoSE project.

Fig. 2 compares the original (ante operam, first column) and new (post operam, second column) configurations of the inlets, and the difference between the original and post-project bathymetries (third column). The main changes around the Lido inlet are the construction of an artificial island in the middle of the channel, the dredging of a new channel behind this new island and the creation of two adjacent safety harbours on the north side of the channel. In the other two inlets (Malamocco and Chioggia), breakwaters have been built in the sea just outside the lagoon (completed in November 2004 and April 2005 respectively) and safety harbours have been created at the sides of the channels. The width of the Chioggia inlet was reduced as the result of the construction of a port for fishing vessels, but the width of Lido and Malamocco has not been alterated Mosquera et al. (2007). The changes also entail modifications to the depths of each inlet, close to where the mobile barriers will be installed at the bottom of each inlet channel. The figure shows that Lido and Chioggia will be deepened; Malamocco inlet will be deepened in the breakwater area, but the depth in the main channel will be reduced.

2.3. *The simulation set-up*

The water column has been discretized into 17 vertical layers with variable thickness ranging from 1 m, in the topmost 10 m, to 7 m for the deepest layer in the outer shelf. The numerical treatment assures the conservation of the total depth, because the bottom layer contains the fractional part of the last layer. This means that the accuracy of the vertical discretization with respect to the changes in the inlets depth is not compromised.
The model was run in fully non-linear mode with the usual finite element discretization for each timestep, the Coriolis parameter being set to the latitude of the central part of the lagoon (45° 25' North). The bottom drag coefficient was set to 0.0045 for the whole domain, and the value of the wind drag coefficient to $2.5 \cdot 10^{-3}$, the same values adopted in Cucco and Umgiesser (2006). All the simulations presented were carried out using a variable timestep with a maximum admissible value of 300 s. For each iteration the choice of the timestep fulfils the Courant stability criteria of the advective and diffusive terms (advective Courant number less than one). The spin-up time of the simulations was 5 days and the initial condition for tidal levels and velocities was 0. The tidal level imposed on the offshore stretch of the Adriatic Sea accounts for the north Adriatic coastal current. A slope of 0.7 cm from the northernmost to the southernmost part of the domain was assumed. This difference in level corresponds to an average coastal current velocity of 0.05-0.1 m s^{-1} in agreement with Gacic et al. (2004); Kovacevic et al. (2004).

In this application, three different scenarios were considered. In the first, the simulations were designed to reproduce tidal circulation, and the only forcing in the model was the astronomical tide calculated at the Lido inlet. In the second and third scenarios, the forcings included real wind velocities (Bora and Sirocco respectively) and tidal levels.

For all scenarios, two different simulations were carried out, considering both the ante operam and post operam numerical grids in order to compare the results obtained. In the first scenario the simulation lasted 90 days, and in the second and third scenario only 60 days. The reason for this choice is that calculating residence times in the first scenario requires long simulations (because of the weak hydrodynamics), while in the second scenario the Bora wind rapidly renews the waters of the lagoon and the simulation used to calculate residence times can thus be shortened. The residence time for the third scenario was not calculated. To evaluate the residence time with real tide and Sirocco wind it would be necessary to find a long enough period characterised by only Sirocco winds, but the mean duration of Sirocco winds in measurements does normally not exceed 24 hours. Moreover, the evaluation of the residence time under ideal Sirocco wind forcing conditions (Cucco and Umgiesser, 2006) indicates that this kind of wind has a residence time between 10 and 15 days. This means that the residence time under Sirocco wind conditions could be calculated only under idealized forcing. Taken together these considerations justify the decision to exclude residence time evaluation for the third scenario.

2.4. The forcing data set

The astronomical tide imposed as the open boundary condition for the first scenario was provided by the ICPSM (the tide-predicting service of Venice municipality) and was calculated at the Lido inlet. The real forcing data set adopted in the second and third scenario, processed by the ICPSM, was collected during 2004 and 2005 at the CNR offshore platform station (15 Km off the Venetian coast) and at the CNR Institute near the historical centre of Venice city.

The wind data used for the real simulation in the year 2005 featured a period of low wind speed of variable direction, followed by a strong Bora event. The first wind period lasted 18 days (maximum wind speed 6 m s^{-1}, average wind speed 1.6 m s^{-1}, main directions 250-280° and -15-30°), while the Bora wind period (maximum wind speed 7 m s^{-1}, average wind speed 2 m s^{-1}) lasted roughly 7 days, from day 23 to day 29. The Bora wind in this period blew for a total of 98 hours, and on days 23, 24 and 25 blew continuously for 3, 19 and 18 hours respectively. The tide level varied between -0.8 and 0.6 m in the first period and between -0.4 and 1 m in the second period.

The wind data used for the real simulation in the year 2004 was characterised by impulsive Sirocco events (maximum wind speed 11 m s^{-1}, average wind speed 3 m s^{-1}) blowing continuously for a maximum period of 9-10 hours.

2.5. Definition of the variables

The numerical simulations focused on the computation of specific variables that were assumed to reflect the inlet modifications. In order to evaluate the effects of the project on the renewal efficiency of the lagoon, the balance of flows through the inlets, water residence times and return flow factor were computed.

The flows were calculated as the average flow between two consecutive neap tides. The fluxes were estimated through the cross sections shown in Fig.1: their positioning ensures that the width of the section was the same under ante operam and post operam conditions. For every scenario we evaluated the sum of incoming (Q_{in}) and outgoing (Q_{out}) flows through each cross section, normalised with respect to the period T considered (for example: $2(\sum(Q_{in}(t)\Delta t)/T\ )$. We calculated the balance between Q_{in} and Q_{out} for both ante operam and post operam scenarios, and the difference between the two. The results obtained give a useful indication of the effects of the new inlet structures on flow dynamics. The second variable considered is the residence time τ, calculated for all the layers of each element of the spatial domain. To compute this we used the method adopted in Cucco and Umgiesser (2006). The tracer initially released inside the lagoon with a concentration of 100% is subject to the action of the tide and wind which drives it out of the basin, leading to a fall in its concentration. The residence time is defined for each element as the time taken to reduce the initial concentration to $1/e$. In this study the residence time in the stretch of sea just outside the lagoon was not calculated. The residence time for each cell on the numerical grid is linked to the renewal time and shows the importance of transport processes. Specifically, comparison of the results obtained for the ante operam and post operam situations can indicate whether the new configuration of the inlets influences the renewal efficiency of the sub-basins and of the lagoon as a whole.

A further variable illustrating the effects of the MoSE project on renewal capacity is the return flow factor b (Sanford et al., 1992). The average residence time of a small and well-mixed embayment is given by:

$$\tau_{av} = \frac{TV_{av}}{(1-b)P} \tag{10}$$

where T is the average tidal period, V_{av} the basin average volume, P the tidal prism or intertidal volume and $1-b$ is the fraction of new water entering the basin during a tidal cycle. The term b is the return flow factor. For each tidal cycle a fraction of the tracer flows out to sea during the ebb tide, but a part of this can flow back into the lagoon again during the next flood tide. The return flow factor gives an estimate of the proportion of lagoon water flowing out to sea that returns to the lagoon with the next flood tide. If $b = 0$ no tracer ejected returns to the lagoon, if $b = 1$ the entire quantity of the tracer returns. The return flow factor has significant effects on residence time. If τ_0 is the residence time for $b = 0$, we obtain from eq. 10:

$$\tau_0 = \frac{TV_{av}}{P} \tag{11}$$

Combining the equations:

$$\tau_{av} = \frac{TV_{av}}{(1-b)P} = \frac{\tau_0}{1-b} \tag{12}$$

This means that it is possible to estimate the return flow factor computing the two residence times τ_{av} and τ_0 independently from the other terms P, T and V_{av}.

Since the residence times are computed for every grid point of the basin, the return flow factor can be calculated for each element of the domain.

$b(x, y)$, where x and y are the coordinates of the domain element, can be expressed as:

$$b(x, y) = \frac{\tau(x, y) - \tau_0(x, y)}{\tau(x, y)} \qquad (13)$$

where $\tau(x, y)$ is the residence time calculated as described above for each element of the domain, and $\tau_0(x, y)$ is the residence time calculated for the situation in which all the tracer that exits the lagoon disappears, so that none re-enters. To calculate $\tau_0(x, y)$ the tracer concentration exiting the lagoon is set to 0. The return flow factor b is used to estimate the effect of tracer return flow on local residence times. Residence time increases when b is higher. Details of its computation can be found in Cucco and Umgiesser (2006). As with residence times, the return flow factor was been calculated for all the layers available for each element.

In order to evaluate the effects on the local hydrodynamic features of the lagoon, the instantaneous and residual currents integrated over all the available layers were calculated, together with the water levels.

To examine the spatial distribution of velocity changes we compared the residual currents in the whole lagoon and around the inlets in every scenario. The residual currents are calculated in accordance with the method described in Umgiesser (2000) and are given as the average residual current calculated from one neap tide to the next.

Finally we compared the time series of water levels and instantaneous velocities at a representative number of sampling points located both inside the lagoon and in the three inlets over the length of the simulations. The sample points discussed in this work are shown in Fig.1. For each station we calculated the determination coefficient R^2, between post and ante operam results together with the root mean square error and scatter index. We also estimated the maximum and minimum differences between post and ante operam water levels and current speeds.

Furthermore the distribution across the spatial domain of the difference in instantaneous current velocities during spring tide in the Bora and in Sirocco scenarios was calculated. This is because hydrodynamic phenomena are stronger during this tidal phase and the results show the maximum intensities. We also verified that the effects during neap tide are similar but less evident.

3. Results and Discussion

3.1. Validation of the hydrodynamic model

The 3-D hydrodynamic model was validated by comparison with measured water fluxes at the inlets. The empirical water discharge data derived from ADCP measurements collected inside each inlet reflected both the influence of tidal and meteorological forcing (Gacic and Solidoro, 2004; Kovacevic et al., 2008). The comparison was 20 days long and was carried out with respect to 2002 and 2004 by adopting the ante operam grid and with respects to 2005 (when the work inside the inlet was almost complete) by using both the ante and post operam grids. The model was found to reproduce the fluxes with good agreement (Tab. 1) in the Lido and Malamocco inlets (R^2 close to 0.9), whereas in the Chioggia inlet the determination coefficient was found to be lower than in the other two inlets. The root mean square error for each inlet is close to 1/10 of the flux value measured through the inlets itself.

The scatter index, which represents the accuracy of the model, ranges from a minimum of 0.22 in Lido to a maximum of 0.42 in Chioggia. The results (Fig. 3) indicate that the model showed a good match with the experimental fluxes at the Malamocco inlet, while yielding slight under-estimates for Lido and slight over-estimates for Chioggia. This outcome confirms that the simulated velocity and other variables modelled in this study using the two grids are realistic.

3.2. Hydrodynamics

The spatial resolution adopted is not fine enough to describe the impacts of the small-scale structures of the mobile gates. It is, however, enough to resolve the larger effects of the main structures, to which the available plans of the project are referred. The results are therefore a small underestimation of the impacts that will take place due to the construction of the mobile barriers.

To evaluate changes in the inlet hydrodynamics both residual and instantaneous water currents and water levels computed during the inflow and outflow of a spring tidal cycle, were considered.

Fig. 4 shows the maps of the residual current with real tide plus Bora wind forcing calculated ante and post operam. It also shows the differences between the post operam and ante operam current speed for each inlet.

Post operam, the residual currents in the Lido inlet are characterised by two new vortices, one behind and the other in front of the artificial island. The position of the main vortex outside the inlet is further north than the situation ante operam. The current intensity is higher along the sides of the island and along the left branch of the main channel. The velocity is higher in other areas just outside the inlet (blue colour), but is lower behind the artificial island and near the seaward end of the south inlet wall (red colour). In the Malamocco inlet, the post operam residual currents include new vortices along the main channel of the inlet, between the breakwater and the seaward end of the inlet and between the breakwater and the coast. The position of the bipolar vortex outside the inlet appears to be further offshore and further north. There is increased current intensity along the main channel, in the areas just outside the inlet (including the outgoing jet) and in the area between the south inlet wall and the coast. The decrease takes place on the seaward side of the breakwater, reaching up to the coast, and between the breakwater and the south wall of the inlet.

In the Chioggia inlet the post operam residual current creates two new vortices: one between the breakwater and the seaward end of the inlet and one on the seaward side of the breakwater. The position of the bipolar vortex appears to be further offshore and further north. The current intensity is higher in the areas just outside the inlet, on the north side of the inlet and near the seawards ends of the inlet walls, whereas it is lower on the seaward side of the breakwater and south of the breakwater.

In all three inlets the maximum increase is 0.15 m s^{-1} and the maximum decrease -0.17 m s^{-1}.

The results for residual current in the astronomical tide scenario are very similar to the results described above for the real tide plus Bora wind scenario.

In the real tide plus Sirocco wind scenario (Fig. 5) the results in the Lido inlet are similar to the Bora scenario. In the Malamocco inlet the main difference is in the area (around 1.7 km) along the coast that shows lower current intensities than with the Bora wind scenario. The most important difference between the Sirocco and Bora scenarios is seen in the Chioggia inlet: the residual current creates only one new vortex (between the dam and the breakwater) and the stream from the south part of the coast flows between the dam and the breakwater, increasing the northward current in front of the inlet.

The results enable us to make three observations: the variation in current intensity in the Lido inlet is a consequence of the new artificial island; the greater post operam depths cannot fully cancel out the effects of narrowing the channel. The increased current intensity in the Malamocco inlet is due to the decreased depth of the channel; and the changes in the current intensities outside the Malamocco and Chioggia inlets can be explained by the presence of the new breakwaters. These alter the residual current flowing northwards (from the south area of the domain) along the coast and split it into two parts: one creates the typical bipolar vortex in front of the inlets and the other flows towards the coast creating a new vortex. A part of this latter residual current flows between the breakwater and the south walls of the inlets and creates new vortices here. Moreover the position of the breakwaters causes the outgoing jet to flow further offshore and further northward.

It is important to note that the changes in residual current are of the same order of magnitude as the original values of the residual currents ante and post operam, so the variations are clearly not negligible.

Post and ante operam timeseries of water levels and instantaneous velocities at various sampling points in the domain were compared for each scenario over the whole duration of the simulations. In this paper only the points inside the inlets shown in Fig. 1 are discussed.

The table 2 shows the statistical analysis of water levels and current speeds. The determination coefficient, root mean square error and scatter index for post and ante operam timeseries were calculated. The last three columns of the table refer to the difference between the post and ante operam timeseries and are named "delta" timeseries. The minimum, maximum and average of the delta timeseries were calculated in order to estimate the maximum range of change for each variable.

The results indicate that the changes in water level are negligible for each inlet and scenario. The current speed shows more significant variations, with similar trends in all scenarios. The lowest determination coefficient was seen at Station 1, positioned behind the artificial island, followed by Stations 2 and 6, located in the left branch of the Lido inlet and the Chioggia inlet respectively. This indicates, especially for Station 1, that the phase of the current timeseries has shifted. The maximum value in the delta timeseries indicates that station 5, situated in Malamocco inlet, has the biggest increase in current speed (0.30-0.40 m s^{-1}) and a moderate decrease (0.10-0.17 m s^{-1}). Stations 6 and 2 see significant changes, with increases and decreases close to 0.20 m s^{-1}. Station 1 sees mainly a decrease. Stations 3 and 4 see changes of approximately 0.10 m s^{-1}. Stations 2, 3 and 6 see symmetrical increases and decreases, whereas Stations 1, 4 and 5 are asymmetrical, with 4 and 5 experiencing a large increase and 1 a strong decrease.

The results obtained from the timeseries analysis clearly depend on the choice of data points. To better evaluate the maximum variation of current speed and the spatial distribution of the changes, we calculated the difference between post and ante operam current speed values in the whole lagoon. Figs. 6 and 7 show the difference during ebb and flood tide assuming maximum spring tide values for Bora and Sirocco wind scenarios respectively.

During the inflow phase in the Lido inlet the current velocity is lower (red) behind the artificial island and in some very shallow areas in the northern part of the lagoon; it increases (blue) on both sides of the artificial island and along the right branch of the inlet up to Venice city. In the Malamocco inlet the current velocity is lower around the breakwater and inside the inlet, reaching across to the landward side of the central basin; it is higher in the seaward part of the inlet channel, in the areas between the coast and the breakwater and in the sea in front of the inlet. The current velocity in the Chioggia inlet is lower around the breakwater and higher in the main channel.

The maximum difference between post and ante operam current velocity in the Bora wind scenario is an increase of 0.68 m s^{-1} and a decrease of -0.94 m s^{-1}. In the Sirocco scenario the values are 0.91 and -0.79 m s^{-1} respectively.

During the outflow phase the current patterns inside the lagoon and in each inlet are similar to the inflow situations, but are generally more extensive. The areas outside the inlets and close to the outgoing jets show an intense change in current velocity, corresponding to the northward shift of the jets and the other effects described for the residual currents. The maximum difference between post and ante operam current velocity in the Bora wind scenario is an increase of 1.13 m s^{-1} and a decrease of -0.93, whereas in the

Sirocco scenario the values are 1.10 and -0.96 m s^{-1} respectively.

The pattern of the current speed timeseries indicates that with the new structures the phase tends to shift only in specific points (e.g., behind the island or in very shallow areas). The differences between maximum instantaneous values of currents velocities during spring tide shown in Figs. 6 and 7 give an idea of the maximum area involved in phase shift, but are not representative of the absolute change. Generally the variations are more intense during outflow than during inflow. The areas inside the lagoon affected by changes during inflow and outflow are similar, whereas outside the lagoon they are located in different areas depending on the wind direction. The order of magnitude of the difference between instantaneous velocities can be up to 1 m s^{-1}, which is comparable to the original instantaneous current velocity values, showing that the described changes are not negligible.

3.3. Residence time

In the northern basin, residence times do not exhibit significant changes in either of the considered scenarios (astronomical tide and real tide plus Bora wind). The new configuration of the inlets leads to a reduction in residence times of about 1-2 days in the central area of the lagoon (Figs. 8 and 9 left). The relative variation in residence times compared to the situation ante operam is shown in the central part of the figures and includes reductions of 3–10%. For example the residence time increases by about 1 day in a small area near the Malamocco inlet. In the astronomical tide scenario the residence time increases by about 1 day on the landward side of the Chioggia sub-basin, which corresponds to an increase of almost 10%.

In both forcing scenarios the return flow factor in the post operam situations is higher in the area from the southern part of the Lido inlet to Venice City (0.01–0.03 in the astronomical tide scenario and up to 0.60 with the real tide plus Bora wind scenario). It is slightly lower in a small area north of the Malamocco inlet and in the northern part of the Lido inlet. In the astronomical tide scenario the return flow factor increases in the inner part of the Chioggia inlet, whereas in the real tide plus Bora wind scenario the return flow factor increases (0.01–0.03) on the landward side of the central basin.

An increase in the return flow factor means that a bigger quantity of tracer returns with the ebb tide. The decrease in residence time and the increase in return flow factor indicate an increase in current intensities and a net improvement in water renewal capacity. Conversely an increase in residence time and a decrease in return flow factor implies that the currents are less intense and that the area is subject to a net worsening in water renewal capacity. The former case is seen in the area between Lido and Venice city, and the latter in the area near the Malamocco inlet. This suggests that the construction of the MoSE structures has the effect of moving the watershed of the Lido sub-basin southwards.

An increase in both residence time and return flow factor is seen in the Chioggia sub-basin in astronomical tide scenario, suggesting that the renewal time of the Chioggia sub-basin is longer with the new structure of the inlet, due to the combined effect of lower current velocities and bigger return flow factors. Table 2 shows the mean value of the delta timeseries (difference between post and ante operam current speeds). The positive but low values suggest that the increased return flow factor plays a more important role in the described effect.

3.4. Exchange flows

From the comparison of the time series of the fluxes through each inlet, a delay in the phase of post operam fluxes in all scenarios is evident. The average values of the delay are close to 400 seconds. For all scenarios the delay of Lido inlet ranges form 384 to 466 seconds, for the Malamocco inlets it varies from 250 to 350 seconds. In the Chioggia inlets the delay has a minimum of 250 seconds in the scenario of tide plus Bora wind and a maximum of 626 seconds in the scenario with only tide.

The difference (post minus ante operam) of the maximum for Lido inlets in all the scenarios varies form 140 to 160 m^3 s^{-1}; for the minimum the difference has a range of -110 to -130 m^3 s^{-1}. For Malamocco inlets the difference of the maximum and of the minimum has range from -470 to -540 m^3 s^{-1} and from 600 to 650 m^3 s^{-1} respectively. For Chioggia inlets the differences for maximum varies from 18 (Sirocco wind) to 45 m^3 s^{-1} and from -48 to -78 m^3 s^{-1} in the case of minimum. The consequence is that in the Lido and Chioggia inlets the signal is amplified, whereas in the Malamocco inlet it is reduced.

For each scenario and each inlet we calculated the balance between incoming and outgoing fluxes in post and ante operam in accordance with the method described in section 2.5, as well as the corresponding difference. Table 3 shows the results.

In the astronomical tide scenario the residual flux through the Lido inlet is incoming and is higher in post operam situation, in the Malamocco inlet the balance is outgoing and is lower and finally in the Chioggia inlet it is outgoing and higher. These results indicate a shift of the Lido watershed towards Malamocco and of the Malamocco watershed towards Chioggia. This implies an enlargement of the Lido sub-basin, a shrinkage of the Chioggia sub-basin and a slightly different position of the Malamocco sub-basin. In the real tide plus Sirocco wind scenario the results confirm these changes, whereas in the real tide plus Bora wind scenario the Malamocco sub-basin enlarges and the other two sub-basins reduce.

4. Conclusions

The implementation of the MoSE project has entailed alterations to the structure of the inlets in the Venice lagoon, with consequences that are both local (affecting the area around the inlets) and lagoon-wide. Our results indicate some of these consequences and make it possible to identify the potential risks and benefits for coastal management.

From model results, the mobile barrier construction does not affect water levels, while small differences can be detected analyzing velocities and a small phase shift is seen analyzing fluxes. The balance of flows through the inlets indicates that the variation affects not so much the overall balance of the lagoon as the relative flows through each inlet. The post operam modifications in the flux balance suggest that each watershed moves southwards. This implies an enlargement of the Lido sub-basin at the expense of the Chioggia sub-basin, whereas the size of the Malamocco sub-basin remains unchanged. The variations in residence time are in agreement with these considerations: the post operam residence time in the southern part of the Lido sub-basin is shorter, corresponding to an increase in current velocity, and in the astronomical tide scenario the residence time increases in the Chioggia sub-basin. The changes in residence time and return flow factor indicate that the causes of these modifications are to be found in both the alteration of the instantaneous current velocity and the new sea-lagoon interaction at the inlets.

The local variation in residual and instantaneous current velocities is a direct consequence of the new structures at the inlets and their new depths thanks to the MoSE project. It is evident that in Malamocco and Chioggia the outer breakwater deviates the jet emerging from the inlet and causes it to travel further offshore; its presence also causes a new circulation involving the seaward end of the inlet itself, the outer breakwater and the stretch of shoreline immediately adjacent to it. One consequence will be the erosion of the old depositional fans outside the inlets and the establishment of a new deposition scheme. An identifiable risk is the trapping of a contaminant between the breakwaters and the coast.

In the Lido inlet the increase in current speed from the southern part of the main channel up to Venice city implies benefits for water renewal but risks for infrastructure conservation.

Acknowledgements

This research was funded by the Osservatorio della Laguna. It was also partially been carried out in the framework of the VECTOR and CMCC projects. The wind data set from the CNR Platform and the tide level time-series were provided by Venice Municipality. The flux data employed to validate the model were provided by Dr. Zaggia L. (ISMAR-CNR). Special thanks to Dr. Sarretta (JRC, Ispra) for technical assistance with the

Geographical Information System and to Dr. Bellafiore and Dr. Ferrarin (ISMAR-CNR) for scientific discussion.

References

Ammerman, A. and McClennen, C., 2000. Saving Venice. Science 289 (5483), 1301–1302.

Bellafiore, D., Umgiesser, G. and Cucco, A., 2008. Modeling the water exchanges between the Venice Lagoon and the Adriatic Sea. Ocean Dynamics 58 (5-6), 397–413.

Bellafiore D. and Umgiesser G., 2010. Hydrodynamic Coastal Processes in the North Adriatic investigated with a 3D Finite Element Model. Ocean Dynamics. Available online.

Bendoricchio, G. and De Boni, G., 2005. A water-quality model for the Lagoon of Venice, Italy. Ecological Modelling 184 (1), 69–81.

Benetazzo, A., 2004. Analisi numerica degli effetti di restringimenti localizzati alle bocche di porto in laguna di Venezia. Atti dell'Istituto Veneto di Scienze, Lettere ed Arti. Venice, Italy II, 423–440.

Berrelli, G., Leuzzi, G. and Purini, R., 2006. Indagine sul sovralzo differenziato indotto della bora nella laguna di Venezia. In: IDRA - 30 Convegno di Idraulica e Costruzioni Idrauliche.

Bras, R., Harleman, D., Rinaldo, A. and Malanotte-Rizzoli, P., 2001. Rescuing Venice from a Watery Grave. Science 291 (5512), 2315–2316.

Cucco, A., Perilli, A., De Falco, G., Ghezzo, M. and Umgiesser, G., 2006. Water circulation and transport timescales in the Gulf of Oristano. Chemistry and Ecology 22 (Suppl. 1), 307–331.

Cucco, A. and Umgiesser, G., 2006. Modeling the Venice Lagoon residence time. Ecological Modelling 193 (1-2), 34–51.

Cucco, A., Umgiesser, G., Ferrarin, C., Perilli, A., Canu, D. M. and Solidoro, C., 2009. Eulerian and lagrangian transport time scales of a tidal active coastal basin. Ecological Modelling 220 (7), 913–922.

Delfina, A., 2004. Alcune considerazioni sulla stima delle dissipazioni di energia prodotte da opere fisse in una bocca lagunare. Atti dell'Istituto Veneto di Scienze, Lettere ed Arti. Venice, Italy II (162), 441–478.

Ferrarin, C., Cucco, A., Umgiesser, G., Bellafiore, D. and Amos, C., 2010. Modeling flux water and sediment between the Venice Lagoon and the Sea. Continental Shelf Research. Available online.

Ferrarin, C. and Umgiesser, G., 2005. Hydrodynamic modeling of a coastal lagoon: The Cabras lagoon in Sardinia, Italy. Ecological Modelling 188 (2-4), 340–357.

Gacic, M., Kovacevic, V., Mazzoldi, A., Paduan, J., Arena, F., Mosquera, I., Gelsi, G., Arcari, G., 2002. Measuring water exchange between the Venetian Lagoon and the open sea. Eos, Trans. 83 (20), 217–221.

Gacic, M., Mosquera, I., Kovacevic, V., Mazzoldi, A., Cardin, V., Arena, F. and Gelsi, G., 2004. Temporal variations of water flow between the Venetian Lagoon and the open sea. Journal Of Marine Systems 51 (1-4), 33–47.

Gacic, M. and Solidoro, C., 2004. Lagoon of Venice - circulation, water exchange and ecosystem functioning - Introduction. Journal Of Marine Systems 51 (1-4), 1–3.

IMAGE - Padua University, 2006. Valutazioni preliminari degli effetti idrodinamici dovuti all'incremento delle resistenze localizzate alle bocche di porto della laguna di Venezia. Tech. Rep. Luglio, IVSSLLAA-CORILA.

Kovacevic, V., Fendi, V., Arena, F., Gacic, M., Mosqueita, I., Zaggia, L., Doná, S., Costa, F., Simionato, F. and Mazzoldi, A., 2008. Water and solid transport estimates through the Venetian Lagoon inlets using acoustic doppler current profilers. In: Scientific Research and Safeguarding of Venice. Research program 2004-2006. 2006 Results. Vol. VI. CORILA, pp. 423–439.

Kovacevic, V., Gacic, M., Mosquera, I., Mazzoldi, A. and Marinetti, S., 2004. HF radar observations in the northern Adriatic: surface current field in front of the Venetian Lagoon. Journal Of Marine Systems 51 (1-4), 95–122.

Maticchio, B., 2004. Effetti idrodinamici prodotti da opere fisse alle bocche di porto della laguna di Venezia. part. I: idrodinamica locale e resistenze idrauliche. Atti dell'Istituto Veneto di Scienze, Lettere ed Arti. Venice, Italy II (162), 287–334.

Melaku Canu, D., 2001. Developing an ecological model for the Lagoon of Venice. Tech. Rep. 244, ISDGM/CNR, Venice.

Molinaroli, E., Guerzoni, S., Sarretta, A., Cucco, A. and Umgiesser, G., 2007. Links between hydrology and sedimentology in the Lagoon of Venice, Italy. Journal of Marine Systems 68 (3-4), 303–317.

Mosquera, I., Gacic, M. and Mazzoldi, A., 2007. Long term changes in the kinematics of the inlets of the Venetian Lagoon (NE Italy). Il Nuovo Cimento 30 (2), 149–156.

Nosengo, N., 2003. Save our city! Nature 424 (5512), 608–608.

Spiro, B. and Rizzardi, S., 2006. Ambiti di tutela. In: Atlante della Laguna - Venezia tra terra e mare. Marsilio editore, pp. 176–180.

Pirazzoli, P. A., 2004. Maree estreme nella laguna di Venezia e variazioni morofologiche alle bocche di porto nel corso degli ultimi due secoli. Atti dell'Istituto Veneto di Scienze, Lettere ed Arti. Venice, Italy II (162), 269–285.

Rosatti, G., Bonaventura, L. and Poli, L., 2002. Analisi dell'impatto del progetto MoSE sulla dinamica e sul trasporto nella laguna di Venezia. In: 28 Convegno di Idraulica e Costruzioni Idrauliche - Potenza, settembre 16-19.

Sanford, L., Boicourt, W., Rives, S., 1992. Model for estimating tidal flushing of small embayments. J. Waterway Port Coastal Ocean Eng. 118 (6), 913–935.

Solidoro, C., Canu, D., Cucco, A. and Umgiesser, G., 2004. A partition of the Venice Lagoon based on physical properties and analysis of general circulation. Journal Of Marine Systems 51 (1-4), 147–160.

Umgiesser, G., 1999. Valutazione degli effetti degli interventi morbidi e diffusi sulla riduzione delle punte di marea a Venezia, Chioggia e Burano. Atti dell'Istituto Veneto di Scienze, Lettere ed Arti. Venice, Italy I (157), 231–286.

Umgiesser, G., 2000. SHYFEM Finite Element Model for Coastal Seas - User Manual - version 4.56, pp 26.

Umgiesser, G., 2004. Effetti idrodinamici prodotti da opere fisse alle bocche di porto della laguna di Venezia. part II: riduzione delle punte di marea ed effetti sul ricambio idrico. Atti dell'Istituto Veneto di Scienze, Lettere ed Arti. Venice, Italy II (162), 335–376.

Umgiesser, G. and Bergamasco, A., 1993. A staggered grid finite element model of the Venice Lagoon. In: Finite Elements in Fluids. Pineridge Press, Barcelona, pp. 659–668.

Umgiesser, G. and Bergamasco, A., 1995. Outline of a Primitive Equations Finite Element Model. Rapporto e Studi, Istituto Veneto of Scienze, Lettere ed Arti XII, 291–320.

Umgiesser, G., Canu, D., Cucco, A., and Solidoro, C., 2004. A finite element model for the Venice Lagoon. Development, set up, calibration and validation. Journal Of Marine Systems 51 (1-4), 123–145.

Umgiesser, G. and Matticchio, B., 2006. Simulating the mobile barrier

(MoSE) operation in the Venice Lagoon, Italy: global sea level rise and its implication for navigation. Ocean Dynamics 56 (3-4), 320–332.

Zemlys, P., Erturk, A. and Razinkovas, A., 2008. 2D finite element ecological model for the Curonian lagoon. Hydrobiologia 611, 167–179.

List of Tables

List of Figures

Table 1:

		2002	
inlet	R^2	RMSE	SI
Lido	0.97	698	0.22
Malamocco	0.95	990	0.27
Chioggia	0.88	834	0.43
		2004	
Lido	0.97	750	0.25
Malamocco	0.95	948	0.27
Chioggia	0.89	749	0.41
	2005	ante operam	
Lido	0.97	787	0.27
Malamocco	0.95	930	0.3
Chioggia	0.92	612	0.34
	2005	post operam	
Lido	0.95	871	0.29
Malamocco	0.92	995	0.33
Chioggia	0.87	771	0.42

Table 2:

		level [m]						speed [m s^{-1}]					
scenario	n	R^2	RMSE	SI	max(delta)	min(delta)	mean(delta)	R^2	RMSE	SI	max(delta)	min(delta)	mean(delta)
	1	1	0.01	0.03	0.01	-0.02	-0.001	0.72	0.03	0.30	0.04	-0.21	-0.01
	2	1	0.01	0.03	0.01	-0.02	-0.001	0.96	0.09	0.22	0.17	-0.16	0.06
astro	3	1	0.01	0.03	0.01	-0.02	-0.001	0.98	0.04	0.11	0.10	-0.09	0.02
	4	1	0.01	0.03	0.01	-0.02	-0.001	0.99	0.04	0.10	0.10	-0.02	0.02
	5	1	0.01	0.03	0.01	-0.02	-0.001	0.98	0.14	0.25	0.30	-0.10	0.12
	6	1	0.01	0.03	0.01	-0.02	-0.001	0.95	0.07	0.14	0.17	-0.19	0.03
	1	1.00	0.01	0.03	0.03	-0.03	-0.001	0.68	0.03	0.30	0.13	-0.22	-0.01
	2	1.00	0.01	0.03	0.03	-0.03	-0.001	0.96	0.09	0.21	0.22	-0.19	0.06
Bora	3	1.00	0.01	0.03	0.03	-0.03	-0.001	0.98	0.04	0.10	0.11	-0.11	0.02
	4	1.00	0.01	0.03	0.03	-0.03	-0.001	0.99	0.03	0.10	0.14	-0.03	0.03
	5	1.00	0.01	0.03	0.03	-0.03	-0.001	0.98	0.15	0.25	0.40	-0.17	0.13
	6	1.00	0.01	0.03	0.03	-0.03	-0.001	0.96	0.07	0.13	0.23	-0.23	0.03
sciro	1	1.00	0.01	0.02	0.02	-0.03	-0.001	0.77	0.03	0.26	0.07	-0.21	-0.01
	2	1.00	0.01	0.02	0.02	-0.03	-0.001	0.96	0.09	0.22	0.22	-0.17	0.07
	3	1.00	0.01	0.02	0.02	-0.03	-0.001	0.98	0.04	0.10	0.13	-0.11	0.02
	4	1.00	0.01	0.02	0.02	-0.03	-0.001	0.99	0.04	0.10	0.13	-0.06	0.03
	5	1.00	0.01	0.02	0.02	-0.03	-0.001	0.98	0.14	0.25	0.35	-0.15	0.12
	6	1.00	0.01	0.02	0.02	-0.03	-0.001	0.96	0.07	0.13	0.26	-0.21	0.03

Table 3:

station	scenario	Lido	Malamocco	Chioggia
Tide	ante	29.6	-29.9	-0.3
	post	35.3	-24.2	-11.1
	difference	5.7	5.7	-10.8
Bora	ante	167.5	-43.4	-124.1
	post	161.7	-32.2	-129.6
	difference	-5.8	11.2	-5.5
Sirocco	ante	-32.9	-56.1	89.0
	post	-19.1	-50.5	69.5
	difference	13.8	5.6	-20.5

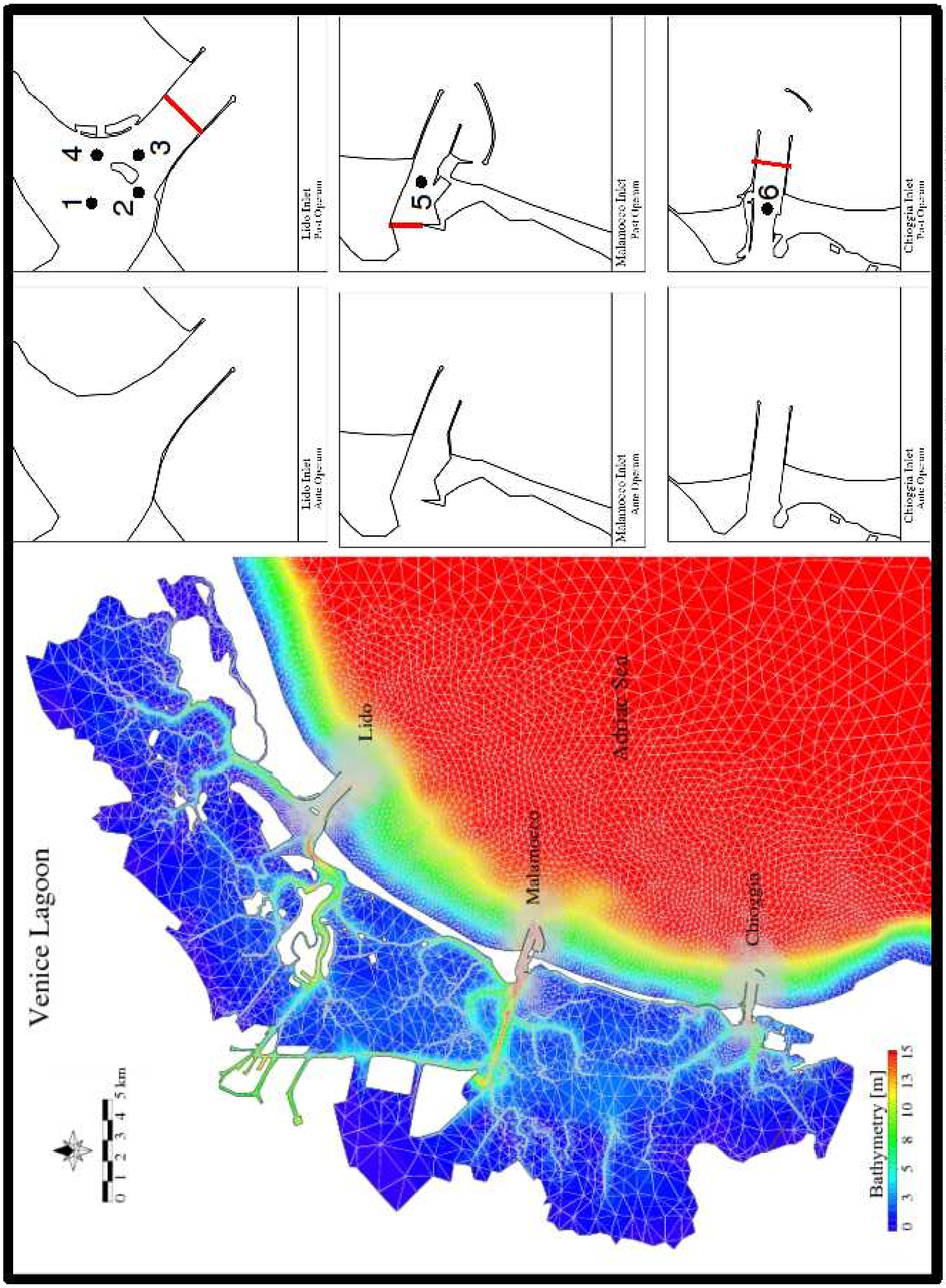
Venice Lagoon
0 1 2 3 4 5 km
Lido
Malamocco
Chioggia
Adriatic Sea
Bathymetry [m]
0 3 5 8 10 13 15
Lido Inlet Ante Operam
Lido Inlet Post Operam
Malamocco Inlet Ante Operam
Malamocco Inlet Post Operam
Chioggia Inlet Ante Operam
Chioggia Inlet Post Operam
1
2
3
4
5
6

Figure 1:

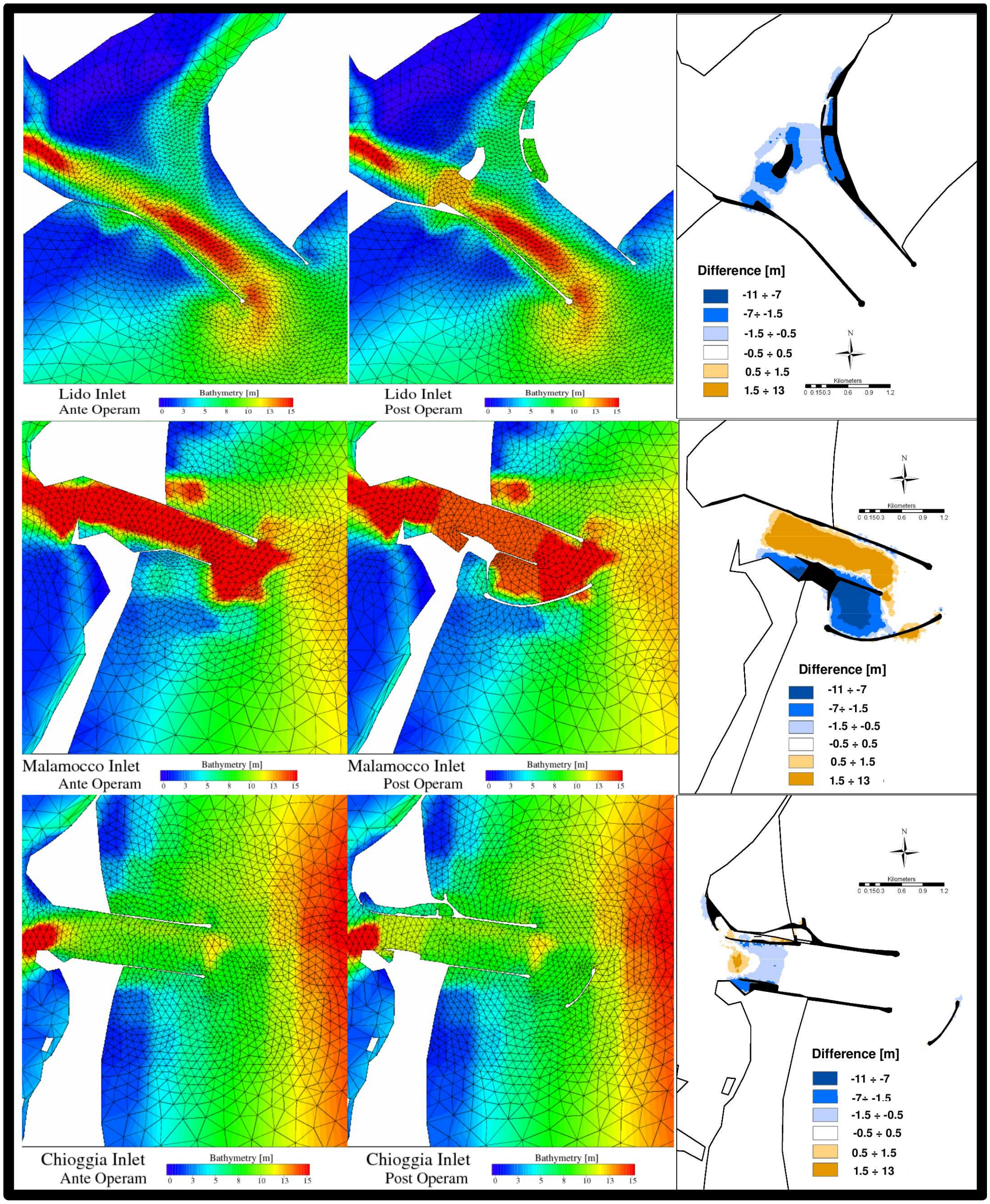
Lido Inlet
Ante Operam
Bathymetry [m]
Lido Inlet
Post Operam
Bathymetry [m]
Difference [m]
-11 ÷ -7
-7÷ -1.5
-1.5 ÷ -0.5
-0.5 ÷ 0.5
0.5 ÷ 1.5
1.5 ÷ 13
N
Malamocco Inlet
Ante Operam
Bathymetry [m]
Malamocco Inlet
Post Operam
Bathymetry [m]
Difference [m]
-11 ÷ -7
-7÷ -1.5
-1.5 ÷ -0.5
-0.5 ÷ 0.5
0.5 ÷ 1.5
1.5 ÷ 13
Chioggia Inlet
Ante Operam
Bathymetry [m]
Chioggia Inlet
Post Operam
Bathymetry [m]
Difference [m]
-11 ÷ -7
-7÷ -1.5
-1.5 ÷ -0.5
-0.5 ÷ 0.5
0.5 ÷ 1.5
1.5 ÷ 13

Figure 2:

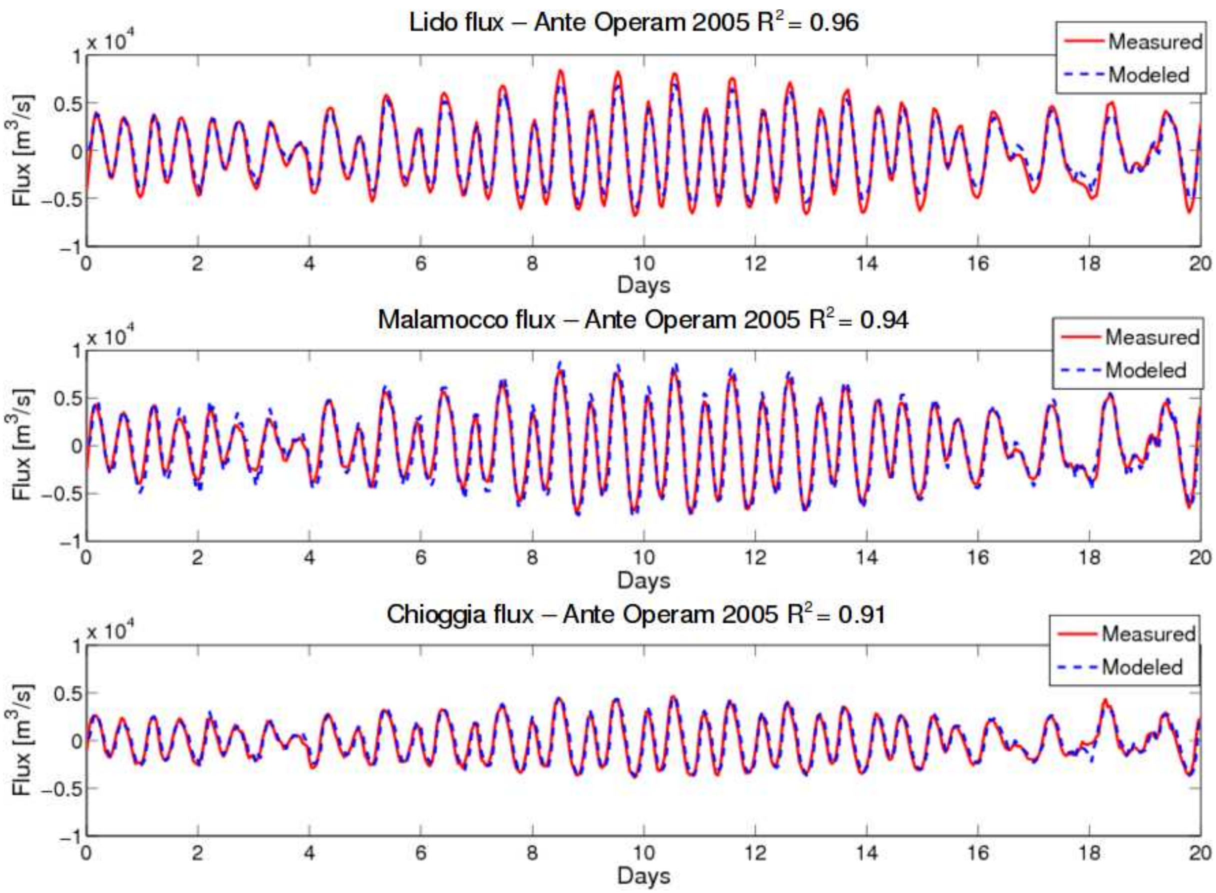

Lido flux – Ante Operam 2005 R² = 0.96
x 10⁴
Flux [m³/s]
Days
Measured
Modeled
Malamocco flux – Ante Operam 2005 R² = 0.94
x 10⁴
Flux [m³/s]
Days
Measured
Modeled
Chioggia flux – Ante Operam 2005 R² = 0.91
x 10⁴
Flux [m³/s]
Days
Measured
Modeled

Figure 3:

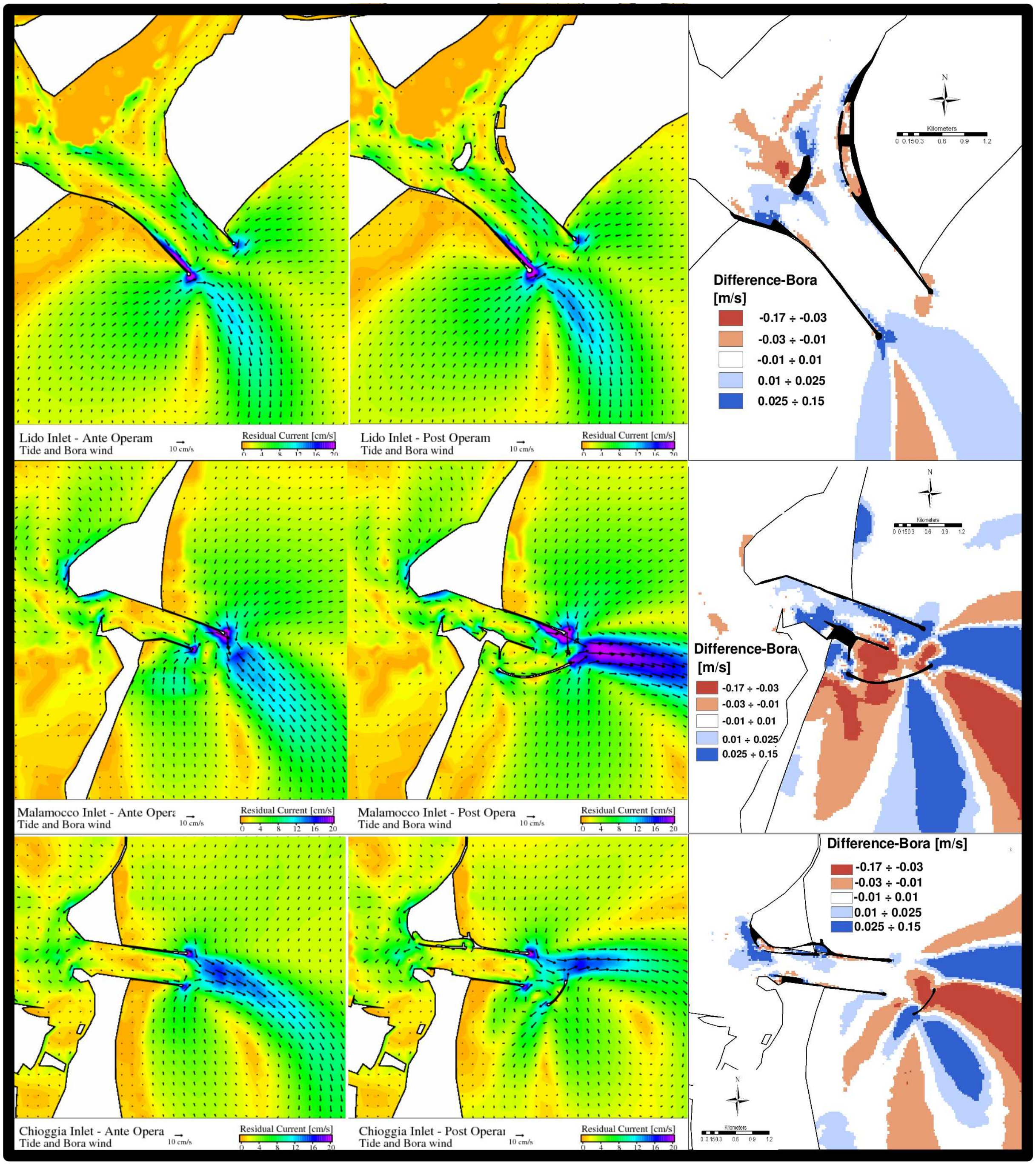
Lido Inlet - Ante Operam
Tide and Bora wind
10 cm/s
Residual Current [cm/s]
Lido Inlet - Post Operam
Tide and Bora wind
Difference-Bora [m/s]
-0.17 ÷ -0.03
-0.03 ÷ -0.01
-0.01 ÷ 0.01
0.01 ÷ 0.025
0.025 ÷ 0.15
Malamocco Inlet - Ante Opera
Malamocco Inlet - Post Opera
Chioggia Inlet - Ante Opera
Chioggia Inlet - Post Operam

Figure 4:

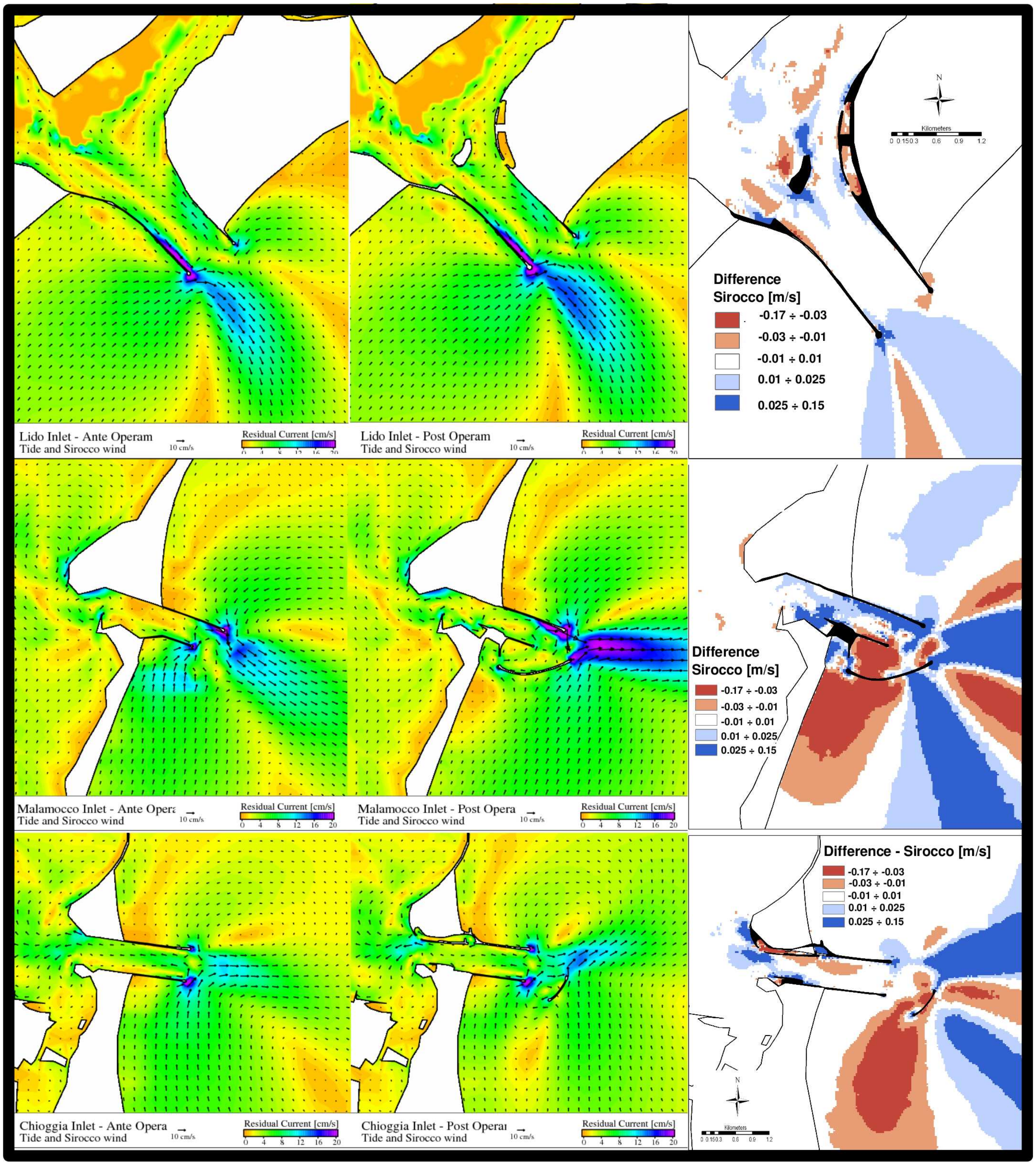

Lido Inlet - Ante Operam
Tide and Sirocco wind
10 cm/s
Residual Current [cm/s]
Lido Inlet - Post Operam
Tide and Sirocco wind
10 cm/s
Residual Current [cm/s]
Difference
Sirocco [m/s]
-0.17 ÷ -0.03
-0.03 ÷ -0.01
-0.01 ÷ 0.01
0.01 ÷ 0.025
0.025 ÷ 0.15
N
Kilometers
Malamocco Inlet - Ante Opera
Tide and Sirocco wind
10 cm/s
Residual Current [cm/s]
0 4 8 12 16 20
Malamocco Inlet - Post Opera
Tide and Sirocco wind
10 cm/s
Residual Current [cm/s]
0 4 8 12 16 20
Difference
Sirocco [m/s]
-0.17 ÷ -0.03
-0.03 ÷ -0.01
-0.01 ÷ 0.01
0.01 ÷ 0.025
0.025 ÷ 0.15
Chioggia Inlet - Ante Opera
Tide and Sirocco wind
10 cm/s
Residual Current [cm/s]
0 4 8 12 16 20
Chioggia Inlet - Post Opera
Tide and Sirocco wind
10 cm/s
Residual Current [cm/s]
0 4 8 12 16 20
Difference - Sirocco [m/s]
-0.17 ÷ -0.03
-0.03 ÷ -0.01
-0.01 ÷ 0.01
0.01 ÷ 0.025
0.025 ÷ 0.15
N
Kilometers

Figure 5:

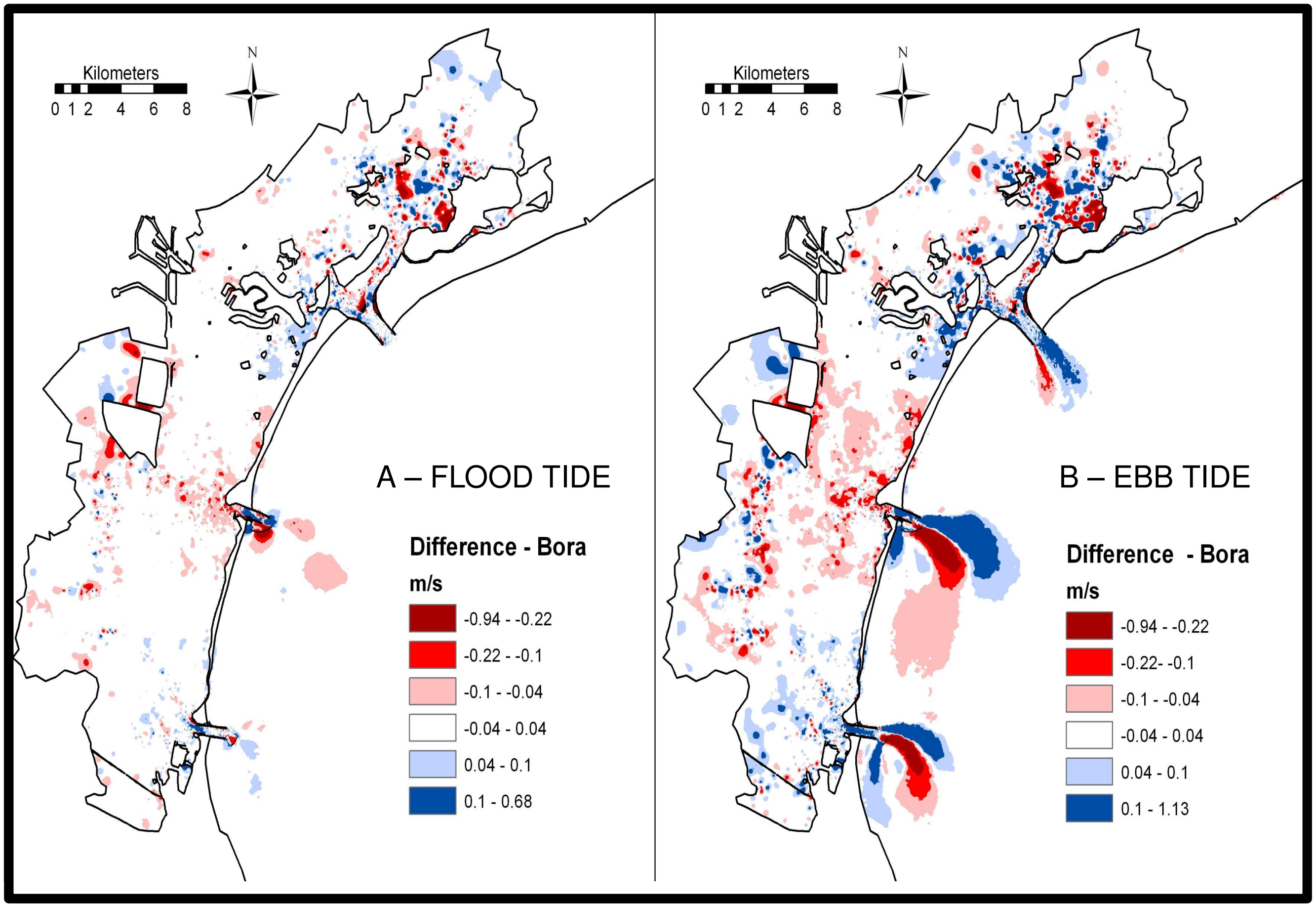
Kilometers
0 1 2 4 6 8
N
A – FLOOD TIDE
Difference - Bora
m/s
-0.94 - -0.22
-0.22 - -0.1
-0.1 - -0.04
-0.04 - 0.04
0.04 - 0.1
0.1 - 0.68
Kilometers
0 1 2 4 6 8
N
B – EBB TIDE
Difference - Bora
m/s
-0.94 - -0.22
-0.22- -0.1
-0.1 - -0.04
-0.04 - 0.04
0.04 - 0.1
0.1 - 1.13

Figure 6:

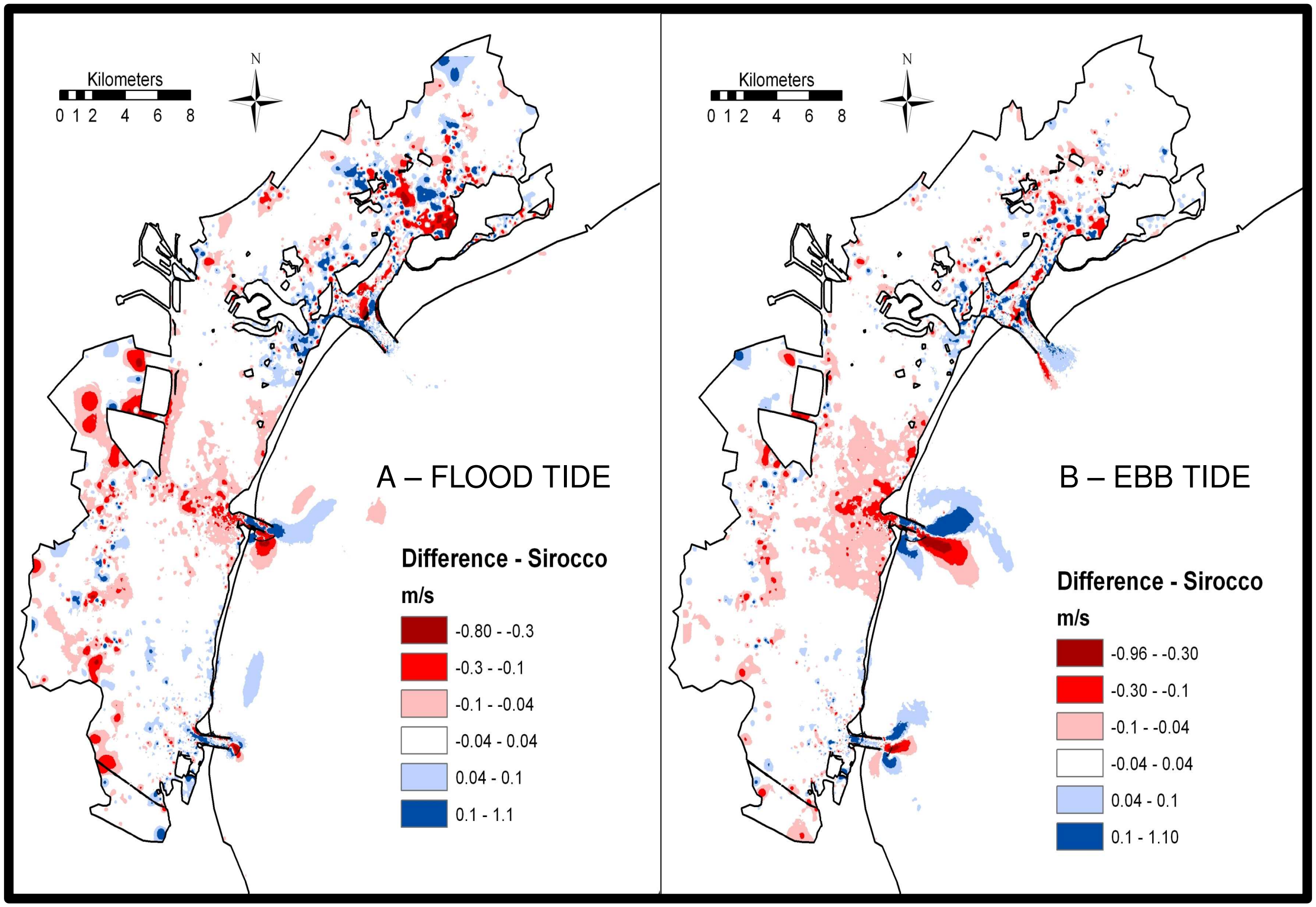
Kilometers
0 1 2 4 6 8
N
A – FLOOD TIDE
Difference - Sirocco
m/s
-0.80 - -0.3
-0.3 - -0.1
-0.1 - -0.04
-0.04 - 0.04
0.04 - 0.1
0.1 - 1.1
Kilometers
0 1 2 4 6 8
N
B – EBB TIDE
Difference - Sirocco
m/s
-0.96 - -0.30
-0.30 - -0.1
-0.1 - -0.04
-0.04 - 0.04
0.04 - 0.1
0.1 - 1.10

Figure 7:

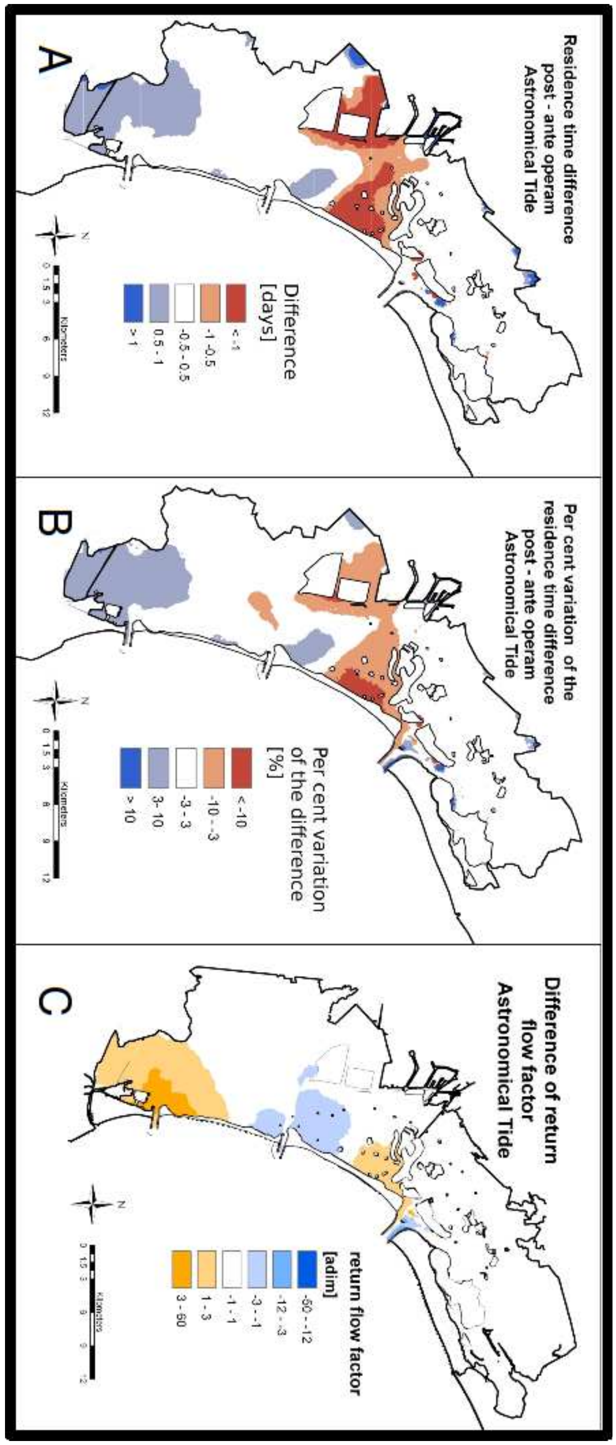
A
Residence time difference post - ante operam Astronomical Tide
Difference [days]
< -1
-1 -0.5
-0.5 - 0.5
0.5 - 1
> 1
B
Per cent variation of the residence time difference post - ante operam Astronomical Tide
Per cent variation of the difference [%]
< -10
-10 - -3
-3 - 3
3 - 10
> 10
C
Difference of return flow factor Astronomical Tide
return flow factor [adim]
-60 - -12
-12 - -3
-3 - -1
-1 - 1
1 - 3
3 - 60

Figure 8:

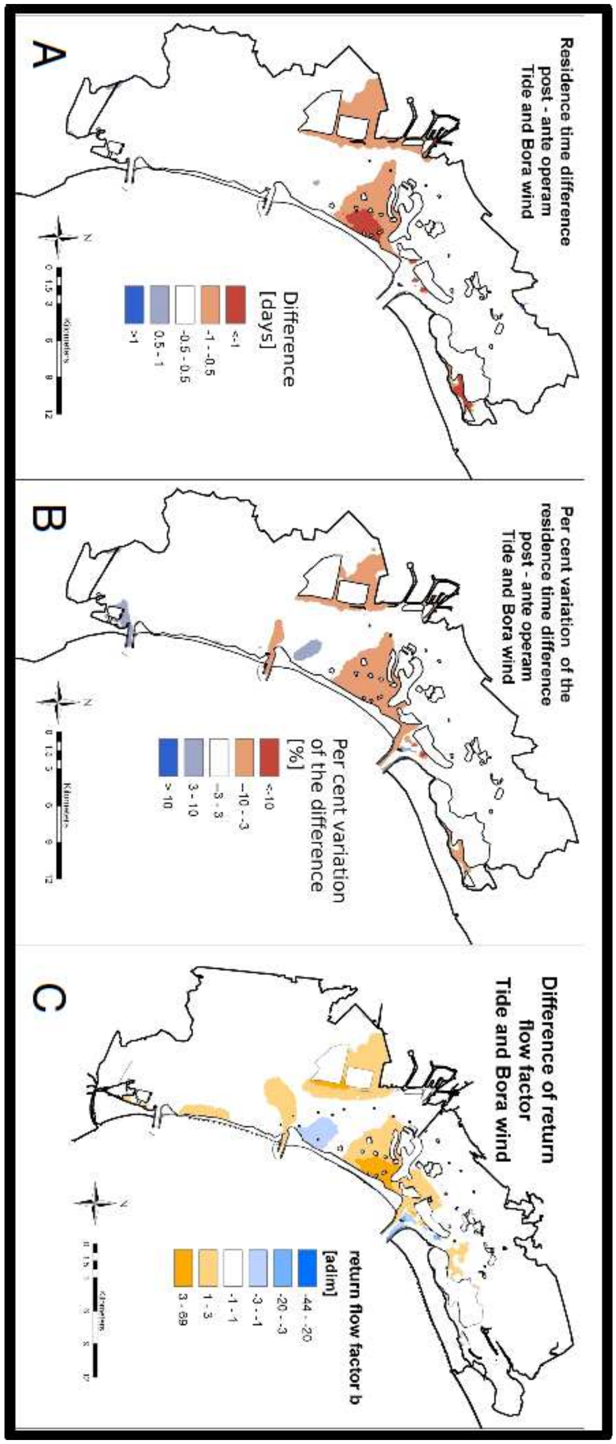
A
Residence time difference
post - ante operam
Tide and Bora wind
Difference
[days]
<-1
-1 - -0.5
-0.5 - 0.5
0.5 - 1
>1
B
Per cent variation of the
residence time difference
post - ante operam
Tide and Bora wind
Per cent variation
of the difference
[%]
<-10
-10 - -3
-3 - 3
3 - 10
> 10
C
Difference of return
flow factor
Tide and Bora wind
return flow factor b
[adim]
-44 - -20
-20 - -3
-3 - -1
-1 - 1
1 - 3
3 - 69

Figure 9: